DOI: https://doi.org/10.24425/amm.2023.141498

C.R. KANNAN[1*], S. SURESH[2], M. NAVANEETHA KRISHNAN[3]

INFLUENCE OF ACOUSTIC EMISSION SIGNALS AND DAMAGE ANALYSIS DURING THE TENSILE TEST ON Al8011 HYBRID COMPOSITES BY STIR CASTING METHOD

Metal network compounds have primary properties. The use of lightweight and low vitality is a testament to the growing interest in the automotive industry. Aluminum alloys, due to their advanced physical, mechanical and tribological properties, have become a highly emerging material for a variety of industrial applications and the importance of efficient material selection is explained. In this paper, an Al8011 hybrid metal matrix composite is developed through the stir casting process. The different weight proportions of B_4C (3%, 6%, 9% & 12%) and fixed proportions of 2% MoS_2 have been used. Composite developed are subjected to mechanical properties evaluation and seawater corrosion studies following standard procedures. To study the porosity of the composite samples, theoretical density and actual density are calculated. An acoustic emission system-assisted tensile test is carried out to report the strength of the composite. From this experimental method, adding reinforcement can increase the tensile strength and hardness of the composites. Under sea water, the increase in reinforcement found an increase in corrosion resistance. Fractured surfaces were perused using SEM and EDS analysis.

Keywords: Al8011; Stir Casting; Acoustic Emission; tensile; corrosion

1. Introduction

The various properties of Al and Al alloys make them excellent candidates for use in the aerospace, defence and automotive industries. High strength along with reasonable ductility is major requirements for such applications. In the past, there has been a continuous effort to enhance the mechanical properties of aluminum alloys through alloying additions, heat treatment, and thermo-mechanical processing. As a well-accepted method of improving the strength of metals and alloys, Metal Matrix Composites (MMCs) have been developed [1]. Aluminium alloy is one of the predominant materials which are used for different engineering applications. The aluminium alloys are suggested for good mechanical properties, corrosion resistance and superior tribological properties [2]. Especially, automobile components such as engine blocks, cylinder walls, power shafts, brakes and gears in miniature size are made of aluminium alloys. Subsequently, the components under severe friction are replaced with modified aluminium alloy [3].

The Aluminium8011 is a wrought alloy that consists of greater strength to weight proportion, better ability to cast and good resistance to corrosion [4]. Al8011 has attractive properties such as good castability, corrosion resistance, and greater strength, etc. [5]. To increase the properties, different reinforcement materials are used. The aluminium alloy with different reinforcements is investigated for different mechanical properties. The reinforcement particles are indifferent forms and wide size variations; they are fiber, whisker, or powder particulate [6]. The most commonly used reinforcement for aluminium matrix is silicon carbide, boron carbide, silicon nitride, alumina, titanium carbide, titanium oxide and other rare earth materials are used [7-11]. There is no doubt that the reinforcement components play an important role in controlling the strength of the hybrid composite [12]. These reinforcements possess maximum wear resistance and are classified under hard materials. With its enormous solidity and low specific mass, B_4C is an incredibly structurally strong monolithic ceramic particle that is more resistant to deformation than SiC [13]. The B_4C and MoS_2 are selected as reinforcements due to their better properties and application compared with others. In particular, B_4C is utilized in transport automobiles, lightarmor, land and airborne because of its greater modulus, minimum density and greater hardness properties [14].

[1] UNIVERSAL COLLEGE OF ENGINEERING AND TECHNOLOGY, DEPARTMENT OF MECHANICAL ENGINEERING, VALLIOOR, TAMILNADU, INDIA
[2] UNIVERSITY COLLEGE OF ENGINEERING, NAGERCOIL, DEPARTMENT OF MECHANICAL ENGINEERING TAMILNADU, INDIA
[3] AMRITA COLLEGE OF ENGINEERING AND TECHNOLOGY, DEPARTMENT OF MECHANICAL ENGINEERING, AMRITAGIRI, ERACHAKULAM (PO), NAGERCOIL, TAMIL NADU, INDIA

* Corresponding author: kannancrk1989@gmail.com

Most composites are fabricated by the stir casting process due to their easiness, better distribution of particles, more production rate and minimum final cost. Higher stirring speeds give a more durable composite than as-cast. The stirrer speed influenced the hardness of a composite during an experiment conducted on it. Increasing the weight percentage of B_4C, and MoS_2 due to the presence of harder reinforcement particles can increase the mechanical properties of the hybrid composite [15]. Al-B_4C-MoS_2 is added as hybrid matrix composites. It has been noted that the addition of molybdenum disulfide in the matrix material has highly influenced reduced wear with good self-lubrication [16]. Sulfur occupies interstitial positions in an oxide layer and slows the reaction between carbon atoms in solid solution and oxide surfaces [17].

Aluminium-based composites are generally fabricated via stir casting and powder metallurgy technique. It is estimated that particle density, size, shape, and volume fraction influence reinforcement settling rates [18]. With the addition of MoS_2 particles, the hardness of the hybrid compounds decreases uniformly. Increasing MoS_2 particle concentration causes the hybrid composites to become more deformable, which leads to a decrease in hardness [19]. Shoufa Liu et al. analyse the tensile strength of Al7075-B_4C-MoS_2 hybrid composites and found that the tensile strength of the composites was enhanced by the B_4C content. The author also reported that this was because of the interfacial bonding and better load transmission mechanism amongst the Al and B_4C-MoS_2. During the yield stage, a large number of AE signals were generated with high amplitudes [20].

In general, the developed composites are directly subjected to mechanical wear and other structural analysis. It is very important to study the mechanical strength of the composite developed [21]. At the same, mechanical testing with Acoustic Emission (AE) setup for metal matrix composite is novel. The research and development of the AE concept have been focused on machining studies and other wear analyses [22]. By incorporating particles into the aluminum alloy, the corrosion characteristics were improved. Process speed and the number of passes, however, lowered corrosion resistance [23].

In this paper, the aluminum-based metal matrix composite is proposed to develop with B_4C and MoS_2as reinforcement. The weight proportion of B_4C is varied and the constant weight proportion of MoS_2 corresponding mechanical strength is evaluated with Al8011 alloy. For better discussion and illustration, mechanical testing of the metal matrix composite has been planned to evaluate along with the acoustic emission setup. The mechanical loading, fracture analysis and acoustic signal/emission analysis on metal matrix composite are very few. Thus, an attempt was made to develop and study the mechanical behaviour of metal matrix composite with an AE system. Despite previous studies of the Al8011 series no attempt has been made to determine the tensile strength using AE in Al8011-B_4C-MoS_2-based hybrid composites.

2. Material and Methods

2.1. Materials and Characterization

The Al8011 wrought aluminium alloy was utilized as the base material and its chemical composition is listed in TABLE 1. The Boron Carbide (B_4C) is in the form of powder (315 nano mesh) and molybdenum disulfide (MoS_2) in the form of powder (300 nano mesh) is used as a reinforcement particle with four different weight percentages to cast metal matrix composite. The chemical composition of B_4C and MoS_2 is listed in TABLE 2 and TABLE 3 respectively. Fig. 1(a) indicates the topographical Scanning Electron Microscope (SEM) image of the Al8011 alloy. The microstructure of B_4C and MoS_2 particles is shown in Fig. 1(b-c). The polygonal form of B_4C elements is identified in Fig. 1(b). It was found that the size range of MoS_2 particles was from 1 to 5 µm.

TABLE 1

Chemical composition of Al8011

Element	Al	Fe	Si	Cu	Mn	Sn	Zn	Ni	Cr	Ti	Others
Weight %	98.13	0.653	0.919	0.013	0.026	0.096	0.01	0.013	0.004	0.019	0.117

TABLE 2

Chemical composition of B_4C

Element	B	C	O	N	Fe	Si	Al	Others
Weight %	75.65	21.8	1.7	0.7	0.05	0.15	0.05	0.5

TABLE 3

Chemical composition of MoS_2

Element	C	O	Mo		S	N	MoS_2/MoO_3	S/Mo
			MoS_2	MoO_3				
Weight %	22.4	13.6	13.0	3.5	26.5	21.1	3.7	1.6

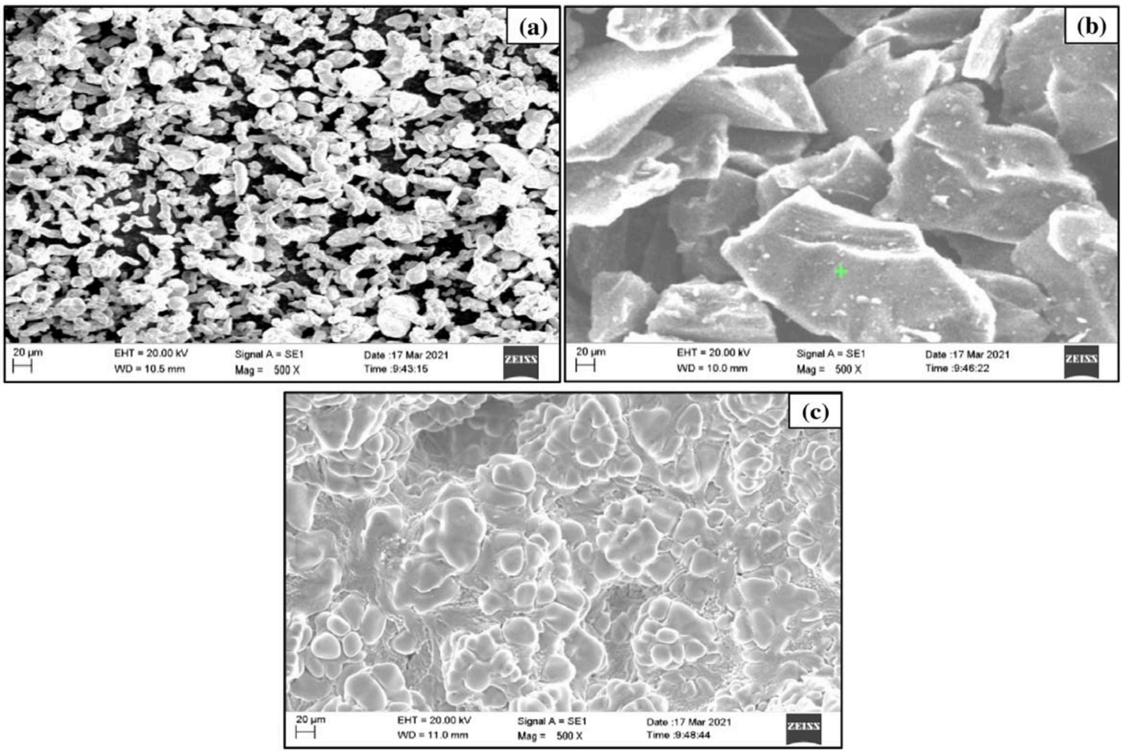

Fig. 1. SEM micrograph (a) Al8011 (b) B_4C powder and (c) MoS_2 powder

2.2. Composite Preparation

During casting, the billet Al8011 alloy is melted in an electric furnace at a temperature of 800°C (±10°C) for a defined proportion. At this temperature, the Al8011 alloy will transform from a solid to a liquid state. The B_4C and MoS_2 particles were preheated to 500°C, then gently added simultaneously to the molten metal, before blending it with matrix material in the stir cast flask. Preheating of reinforcement will help to get a uniform dispersion and gradual heat gradient in the furnace during stirring. The preheated B_4C and MoS_2 are added to the crucible and started to stir at a speed of 350 rpm for 4 minutes, for complete dispersion of reinforcement on the fused matrix material. Fig. 2 shows the stir casting setup used in the stir casting process while making a metal matrix composite with Al8011 alloy and B_4C-MoS_2 as reinforcement. The cast material in the molten state is transferred to a cylindrical metal die (250×25 mm) and allowed to solidify at room temperature. The same procedure was followed to cast the composite with different weight proportions of reinforcement. The size of the composite casting was designed based on the requirement of all microstructural and mechanical tests. The specimens for SEM microstructure analysis were prepared to the required size with the help of wire cut EDM and polished with 300, 600, 1200 and 2000 grit emery sheets. Finally, the diamond paste is used to get the mirror finish surface for SEM analysis.

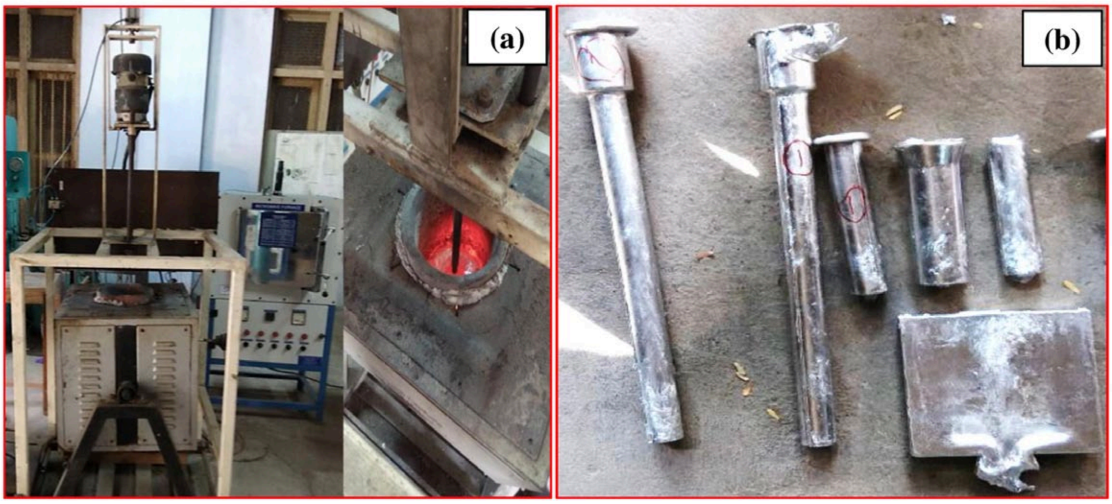

Fig. 2. (a) Stir casting setup used for casting and (b) Cast Specimen

2.3. Characterization of composites

The microstructure of the developed composites was analyzed through an SEM and EDS to identify the distribution of reinforcement particles in the aluminium matrix material. Fig. 3(a-e) shows the SEM image of the Al8011-B_4C-MoS_2 composite. From Fig. 3(a-e), it can be identified that the B_4C & MoS_2 reinforcement distribution in the aluminium matrix is reasonably uniform without the particle clusters. The image with a minimum dark zone reveals the minimum porosity formation level in the specimen. The defects in casting and effects of shrinkages were not identified from the SEM results. The matrix and reinforcement particles were held in the melt for a long duration. This is the reason for uniform dispersion. The preheating of B_4C and MoS_2 powders and the dual stirring process enhances the wettability and reduce the agglomerations by removing the gaseous layers.

Fig. 4(a-e) indicates the EDS mapping of Al8011-B_4C (3, 6, 9 & 12%)-2%MoS_2 composites. It confirms that Al, B, C, Mo and along chemical elements are present in the composites. Fig. 4(a-e) as well affirms the good distribution of B_4C and MoS_2 elements in the composites.

2.4. Experimentation

2.4.1. Hardness

The microhardness test was carried out following the standard test method on polished specimens of Al 8011 alloy and its alloys. The hardness of the composite was measured using Vicker's micro-hardness tester according to ASTM A370. All samples were used for 10 s with a load of 500 g. Five different locations were chosen to avoid any impact on the hard

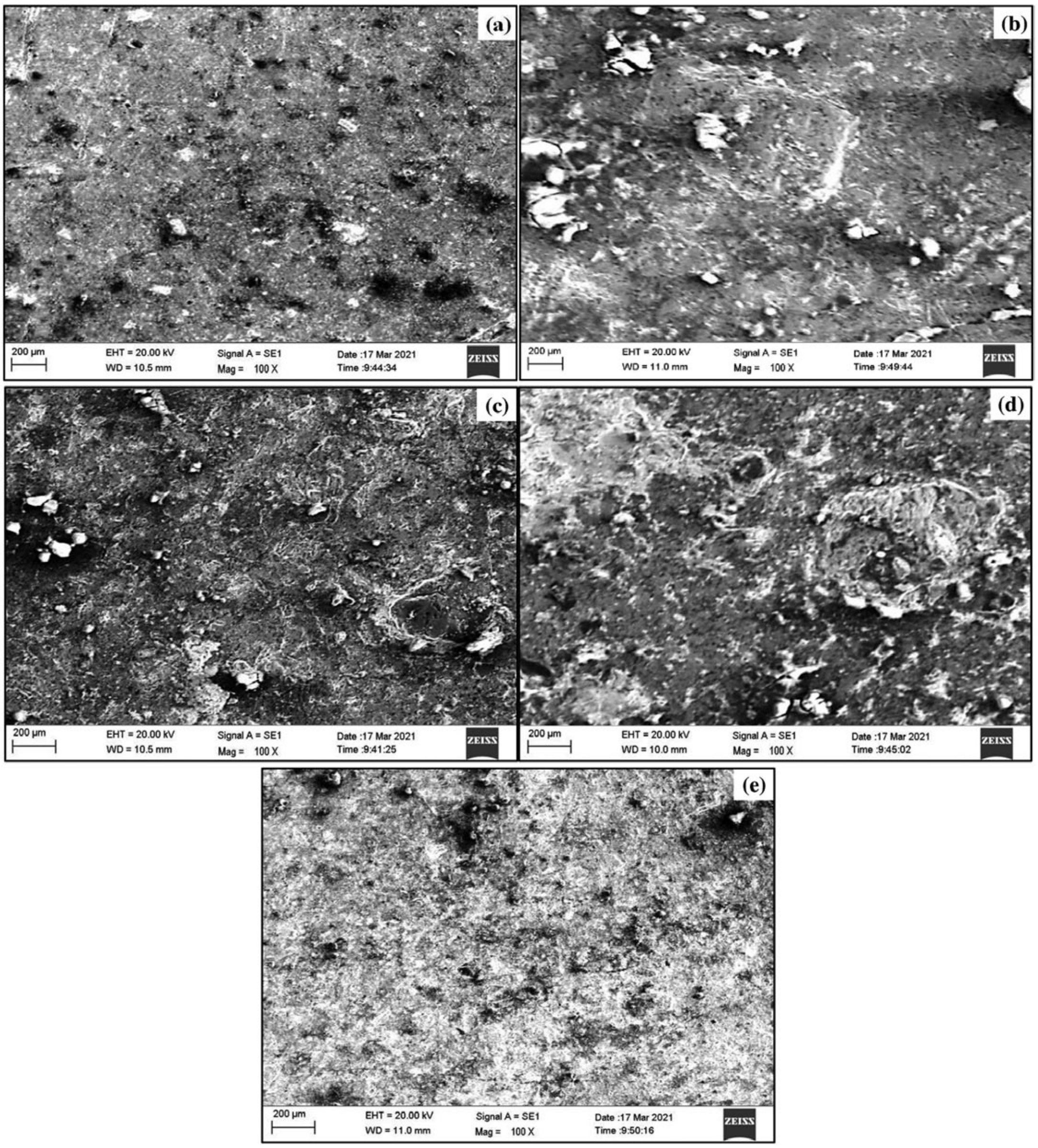

Fig. 3. SEM micrograph of composites (a) Al8011 (b) Al8011-3%B_4C-2%MoS_2 (c) Al8011-6%B_4C-2%MoS_2 (d) Al8011-9%B_4C-2%MoS_2 and (e) Al8011-12%B_4C-2%MoS_2

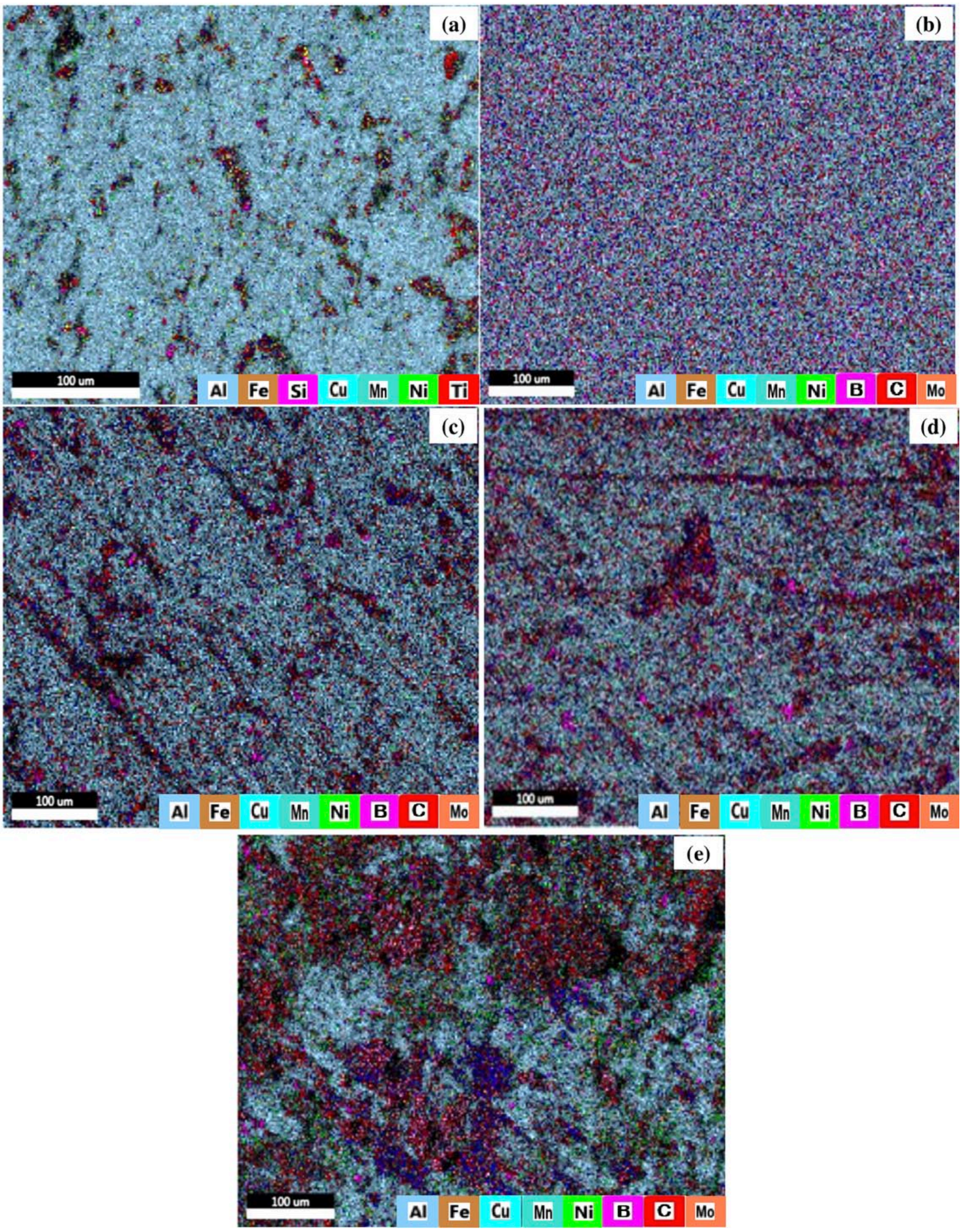

Fig. 4. EDS mapping of composites (a) Al8011 (b) Al8011-3%B_4C-2%MoS_2 (c) Al8011-6%B_4C-2%MoS_2 (d) Al8011-9%B_4C-2%MoS_2 and (e) Al8011-12%B_4C-2%MoS_2

reinforcement particles caused by indentation. The mean of all five readings was plotted in a graph chart.

2.4.2. Density and Porosity Measurement

Theoretical density and actual density of the composite material compared to the quality of the MMC material created. To check the observational density of the developed composite, the castings were polished and Archimedes' principle was applied. In addition, the theoretical density of the composite material is calculated based on its volume fraction so that a better understanding can be achieved. The porosity was evaluated using the actual and theoretical density of the composites [18].

2.4.3. Tensile test

A tensile test of a material is generally performed to determine the tensile properties such as limit of proportionality, yield point, maximum tensile strength, breaking strength, % of elongation, % of reduction in area and modulus of rigidity. The

1200 grit grindings silicon carbide paper turned into used to shine the take a look at specimens if you want to lower the machining scratches and the results of surface defects at the sample. The raw stir cast, metal matrix composite is machined to a standard tensile test sample shape in the machining center (CNC Lathe). The dimensions of the tensile test sample followed the ASTM E8 standard as shown in Fig. 5. Ensuring the standard dimensions, the test samples are investigated with the Instron UTM machine embedded with AE data recording systems. AE signals derived from tensile tests are compared with the tensile observations concerning the designed composite material. Five sets of specimens were prepared to conduct the test [24].

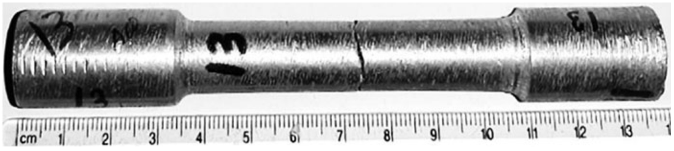

Fig. 5. Tensile test sample as per the Standard ASTM E8

2.4.4. Acoustic emission testing

The sound emission technique is used to study the dislocation or deformation of the object due to mechanical loading. AE systems are used to measure the energy released by the specimen during deformation, and the analysis of the material's characteristics yields more reliable information than theoretical calculations, especially when dealing with heterogeneous materials [11]. The variation in object fracture is confirmed by the signal produced during the mechanical loading. The signals will be in the form of waves developed at a local (fracture zone) due to transient energy [25]. The schematic illustration of the AE system with the UTM test machine is shown in Fig. 6. The piezoelectric-micro 80 model sensor with 250 kHz resonance frequency capacity AE is used for the measurement. The frequency response of AE is 10 kHz-2.1 MHz ± 1.0 db. The prepared specimen is mounted between the holding grip of the UNITEK-94100 and the AE Recorder is fixed in the middle of the sample.

The tensile testing machine is capable of measuring the instantaneous applied load and tensile stress behavior of the sample, extending the sample continuously and simultaneously at a constant rate of 30 mm/min. But the experiments were carried out at room temperature with a low crosshead speed of 0.5 mm/min as detailed. Every nanosecond is recorded on an AE recorder and graphs are generated with yield load, ultimate load and breaking load. This will provide 50% more accurate failure predictions, especially in identifying the initial point of cracking in samples. The various AE parameters obtained from the test setup are via count, duration, hits, energy, event, etc. AE counts are generated from the comparator only when the AE signal exceeds a given limit value, which can further avoid unwanted noise and signals.

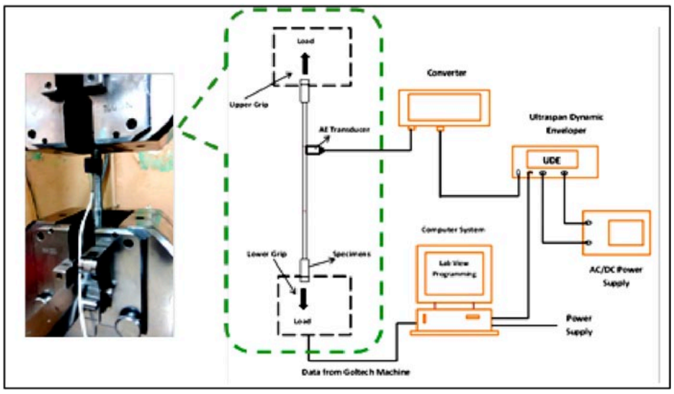

Fig. 6. Block diagram for UTM test machine interconnected with acoustic emission facility

2.4.5. Corrosion analysis through the immersion method

The behaviour of the material under seawater was studied for material loss due to corrosion. For the investigation, clean seawater is collected to study the surface behavior of the composite under the immersion technique. The experiments are planned for immersion studies with the ASTM procedure. Each sample is metallurgically polished; the initial weight is measured and then immersed in seawater separately. After 250 h the samples are drained from the beaker and washed in clean water and air-dried to remove the salt deposits. Corrosion rate measurements reveal that corrosion rate is decreased with increasing garnet percentage [33]. The weight in the samples is measured at last and the corresponding corrosion rate is computed empirically using the formula (Eq. 1)

$$Corrosion\,rate\left(Cr\right)=\frac{534W}{DAT}\left(\frac{\text{mm}}{\text{yr}}\right) \quad (1)$$

Where; W is the weight of Specimen (mg), D – density of the Composite (g/cc), A – total surface area revealed to the seawater for a time duration T.

3. Results and discussion

From the test, developed composites made with reinforcement material at different weight ratios are evaluated according to ASTM standards by the stir casting method. The results achieved for the composite are balanced by the commercially available Al8011 alloy for healthy discussion.

3.1. Effect of hardness, density and porosity

The results of the microhardness tests were conducted on the prepared composite containing different wt. % of B_4C and MoS_2 particles are shown in Fig. 7. The Al8011 contains the minimum hardness value of 50HV. The hardness of composite specimens gradually increased with an increasing percentage

doi:10.1016/j.matlet.2009.11.032

of powders incorporating B_4C and MoS_2 into the metal matrix. The composites containing 3, 6, 9 and 12% B_4C with Al8011-2% MoS_2 have a hardness of 62.5HV, 76.4HV, 83.6HV and 89.5HV respectively. The B_4C has a higher hardness and its existence in the Al matrix further increases the composite's hardness. Adding reinforcement to the Al matrix increases the hardness of the composite. Al8011-Amongst the MMCs fabricated, composite reinforced with 12%B_4C and 2%MoS_2 has a superior hardness value (89.5HV). From Fig. 7, it can be noted that MMC hardness increases with an increase in B_4C percentage [26].An increase in hardness of the MMC with reinforcement addition may attribute to the higher hardness value of reinforced B_4C. It is an experimentally proven fact that whenever a hard reinforcement is incorporated into a soft ductile matrix, the hardness of the matrix material is enhanced. It is a result of the high hardness property of B_4C & MoS_2 and the uniform distribution of reinforcement particles within the Al matrix. Many other researchers have observed similar trends [15,27,28].

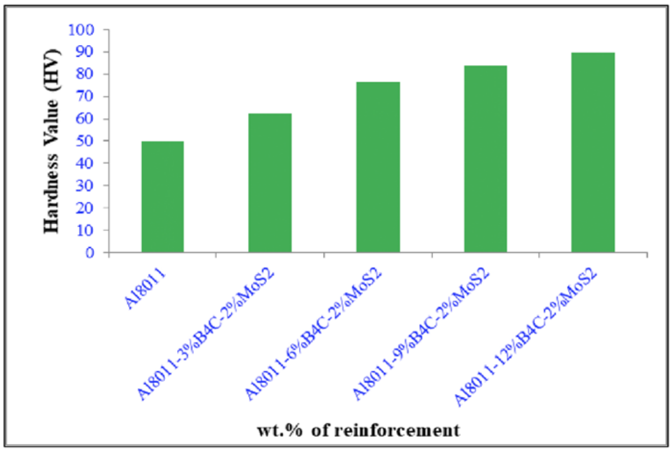

Fig. 7. Hardness effect on Al-B_4C-MoS_2 composites

The density of the composite is found to decrease with an increase in reinforcement due to the minimum density of reinforcements (B_4C and MoS_2). The size of B_4C and MoS_2 particles also has a considerable effect on decreasing density and as the particle size decrease, the density also decreases. Fig. 8 shows the density of the reinforced composite developed through the stir casting route. The density of the composite was found to decrease in trend and itis due to the influence of the B_4C and MoS_2, addedat different proportions in the matrix material. The results are significant to the actual material property. Especially, the actual density of the stir cast metal matrix composite found slight decreases than the theoretical density value. The significant reason for the changes in actual density is that the aluminium alloy light in weight will be metallurgically fused with the reinforcement, which has high solubility to form a perfect composite and the presence of voids.

The aluminium alloy will react with B_4C and MoS_2 and the reinforcement helps to cover the maximum surface of the grains. Because of this, a combination of Al8011-B_4C-MoS_2 will support to reduction of voids/porosity and perfect composites are

Fig. 8. The theoretical andactual density of the Al8011-B_4C-MoS_2 composites

developed. To confirm this claim, the difference in density (actual and theoretical) is used to measure the porosity and is planned as well in Fig. 9. It is clear to confirm that the composite developed through stir casting has allowable porosity (approximately 5%) and it has been reduced with an average amount of reinforcement. Therefore, concerning the density and porosity results, the composite developed with 9% and 12% B_4C has produced good results compared to other weight proportions. Several other researchers have observed similar trends [18].

Fig. 9. Porosity in the Al8011-B_4C-MoS_2 composites

3.2. Effect of tensile strength

As the reinforcement in the metal matrix was added to the matrix and the weight percentage increased, the ultimate strength increased gradually. The maximum Tensile strength was observed at 12%B_4C-2%MoS_2. As the reinforcements are added, the particulate reinforcements form nuclei resulting in more grains will form. Thus, the movement is further controlled, which results in greater. The deformation of the composite concerning tensile load, detected from the tensile test is plotted in Fig. 10. The pure Al8011 is a soft ductile material and plastically deformed to a maximum length and peak load of 15.4 mm and 12.35 kN respectively. The composition of 3% and 6% B_4C with 2% MoS_2 contains the maximum load of 13.125 kN and 13.565 kN during the test and its deformation has 14.200 mm and 12.300 mm. Composites have better mechanical properties than aluminium due to the presence of B_4C and MoS_2 particles in the Al matrix. Since the alloy is a soft ductile material, it has been plastically deformed with an average load. Similarly, the composite with the reinforcement of 9% and 12% B_4C with 2% MoS_2 has sustained a maximum load of 14.715 kN and 18.842 kN during the investigation. The corresponding deformation has a significant scale of 9.400 mm and 8.400 mm to pure alloy. Corresponding fracture load is maximum, ultimate stress found increased and the rate elongation is reduced with these combinations of reinforcements. The rapid fracture was found with the minimum reinforcement percentage. The reason for the short failure is that B_4C & MoS_2 have a better bonding and reduced porosity than other compositions. The low percentage has made the composite metallurgically inferior and the fractured surfaces are analyzed in detail. Findings in this study corroborate those in earlier studies [21,24].

3.2.1. SEM and EDS analysis of Al8011-B_4C-MoS_2 composite during tensile loading

The tensile specimens were analyzed using a scanning electron microscope (SEM) and Energy EDS analysis to understand the fracture mechanics of the developed composite material. Fig. 11 shows the fractography results of the composite observed at two different magnifications. The reinforcement with 0% B_4C and MoS_2 shows the surface morphology of regular ductile fracture. The soft matrix material has been yielded with a dimple

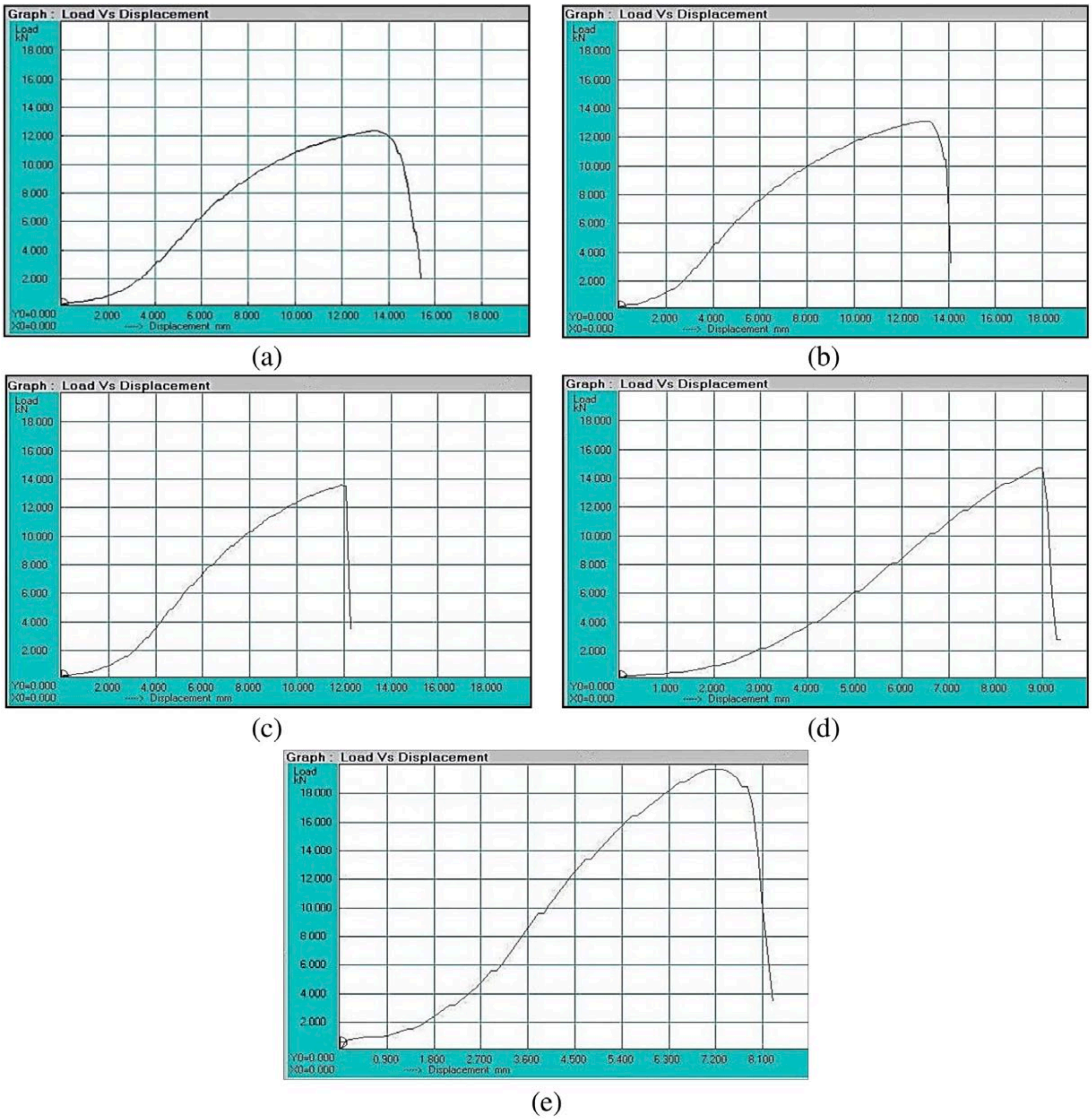

Fig. 10.Observations on Load – Displacement during tensile loading of Al8011-B_4C-MoS_2 composites. (a) Al8011 (b) Al8011-3%B_4C-2%MoS_2 (c) Al8011-6%B_4C-2%MoS_2 (d) Al8011-9%B_4C-2%MoS_2 and (e) Al8011-12%B_4C-2%MoS_2

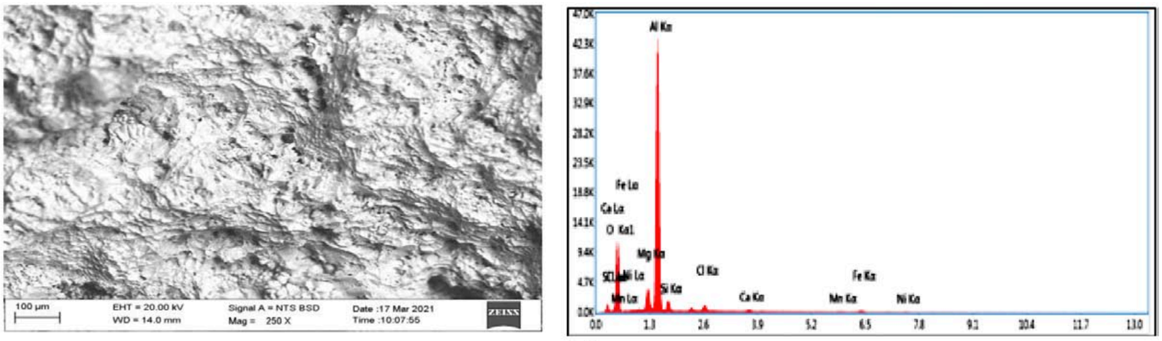

(a)

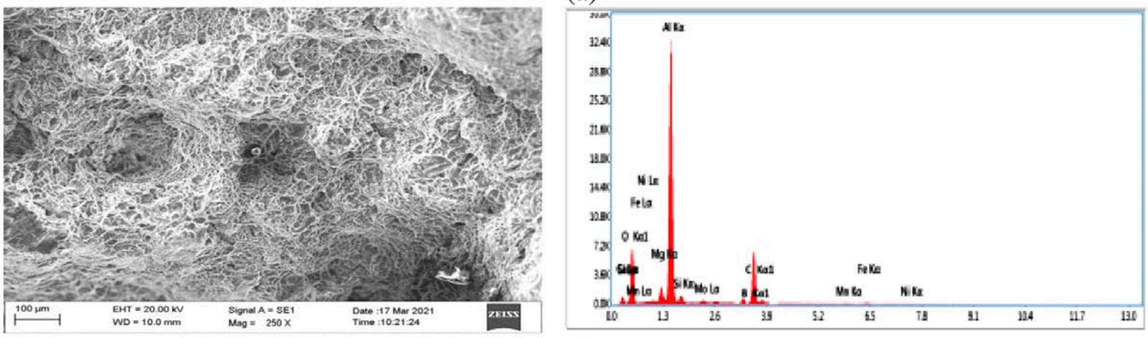

(b)

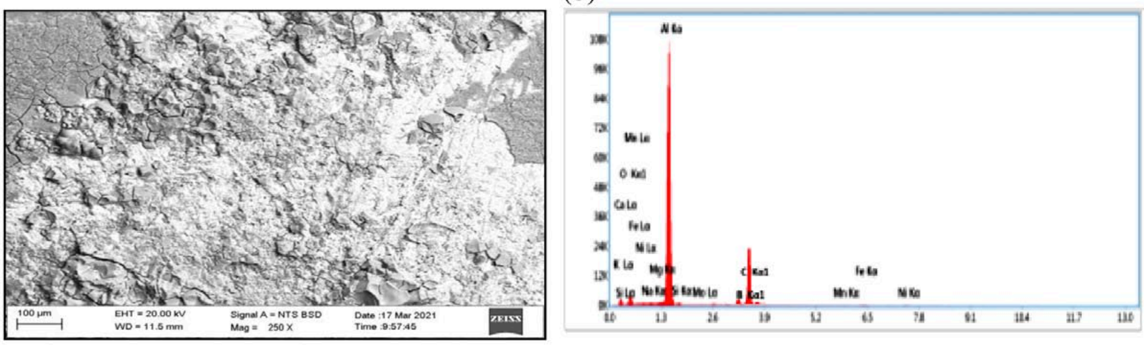

(c)

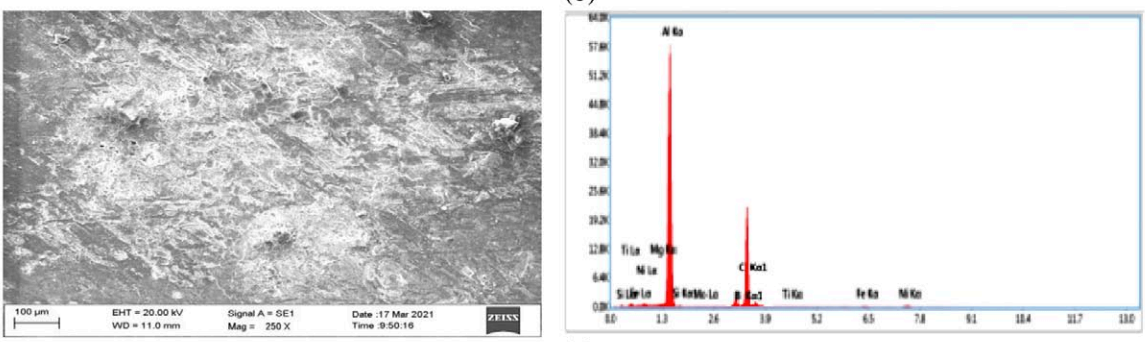

(d)

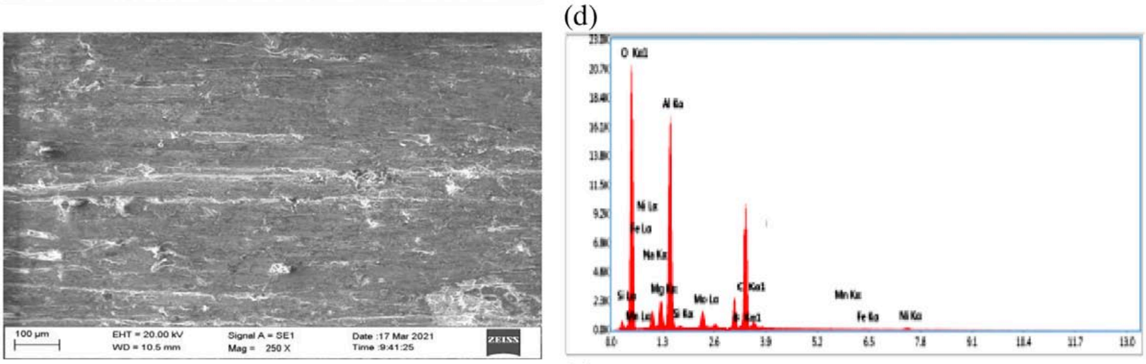

(e)

Fig. 11. SEM and EDS results of Al8011-B_4C-MoS_2 composite during tensile loading (a) Al8011 (b) Al8011-3%B_4C-2%MoS_2 (c) Al8011-6%B_4C-2%MoS_2 (d) Al8011-9%B_4C-2%MoS_2 and (e) Al8011-12%B_4C-2%MoS_2

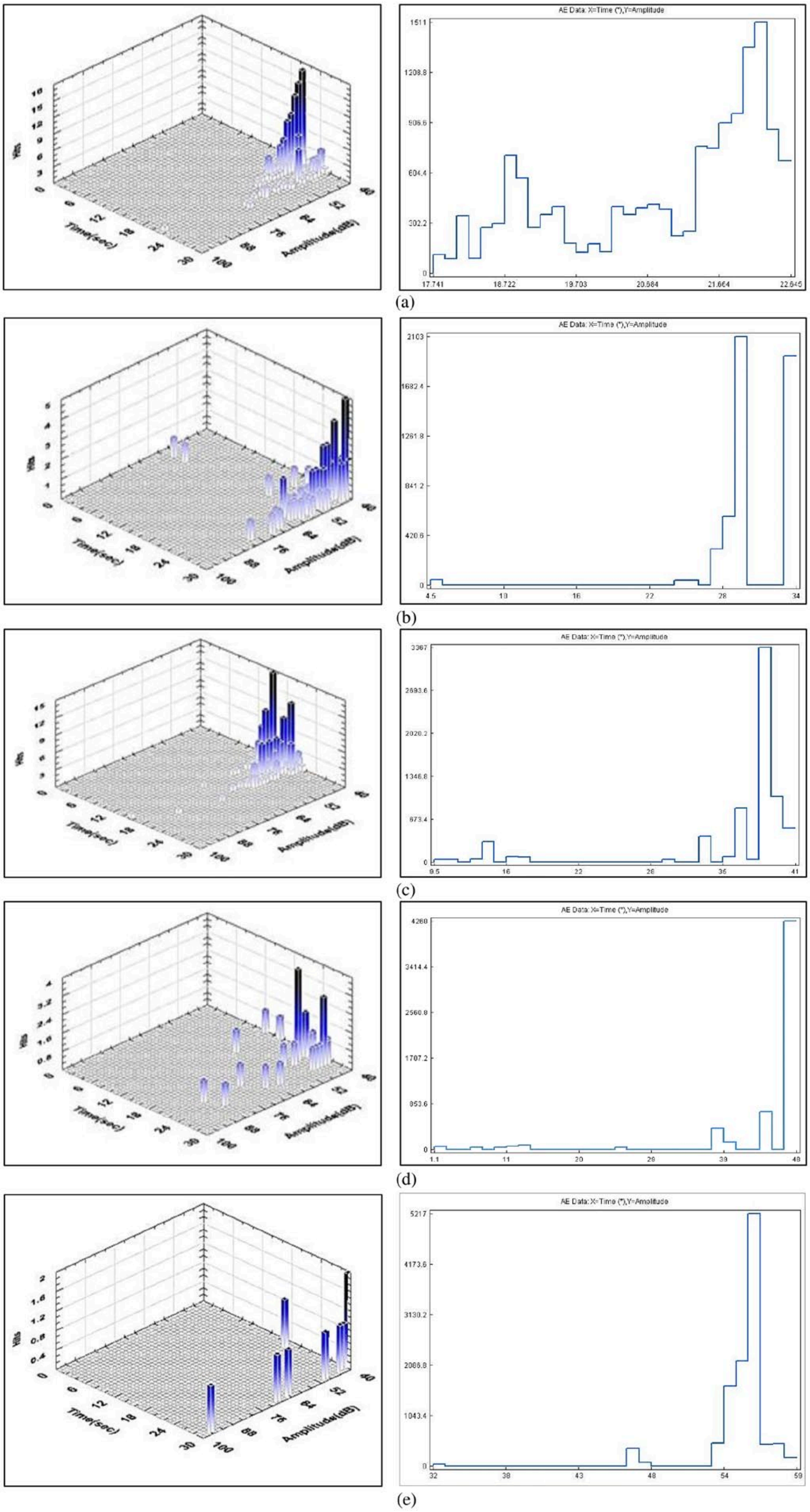

Fig. 12. AE report on 3D profile graph (Time-Hits) and AE Data graph (Time-Amplitude) (a) Al8011 (b) Al8011-3%B_4C-2%MoS_2 (c) Al8011-6%B_4C-2%MoS_2 (d) Al8011-9%B_4C-2%MoS_2 and (e) Al8011-12%B_4C-2%MoS_2

profile during fracture on tensile load conditions and this is called a pure ductile fracture mechanism.

While developing the material with reinforcements, the nature of the composite varies concerning the properties of reinforcement, cast method and its process conditions. During solidification, the reinforcement will be highly influenced by the matrix material. In this occurrence, the grain nucleation, rate of growth, coalescence of voids, reinforcement pull out, agglomeration, crack growth and propagation can be seen in the fractured area of the sample. This is due to the presence of B_4C and MoS_2 (wt.%) reinforcement particles along the grain and the boundaries of the matrix material. Fig. 11 confirms that the fracture is ductile. In particular, aluminium is inferior to hard/dense reinforcements and sudden transformation occurs during solidification. It has been observed with the maximum weight percentage of reinforcement particles (12%B_4C-2%MoS_2). Thus, both brittle and ductile fracture mechanism plays a vital role in the composite material and possesses high strength before fracture. As with earlier studies, these results are consistent [29]. To discuss in detail, the signals recorded with the AE systems during tensile loading are applied to correlate.

3.3. AE report on 3D profile graph and the changes in amplitude

According to the acoustic emission studies, the deflections in the tensile test samples are observed in detail and the data are recorded from the system of the Physical Acoustic Corporation (PAC). The ambient noise is filtered up to 40 dB and frequency of 10 kHz to 2.1 MHz. The PAC sensor (with high resonance) is used to connect test samples with silicon paste/grease. As a result, the deflections in the samples are observed concerning time, amplitude, counts and hits. 3D profile graph and the changes in amplitude are represented in Fig. 12. For pure aluminium alloy samples, the material faced pure ductile transition and the amplitude during the fracture was found to deviate with time in a wide range. This is due to that the Al alloy will fail before the yield and metallurgical fracture. The maximum amplitude for the pure material is up to 1511 dB.

However, with an increase in the weight percentage of the B_4C and MoS_2, there were drastic changes in amplitude at a failure point. Fig. 12 shows the time vs hits. It is verified by the signal that cracks are triggered slowly when the composite material is strong and long-lasting. Therefore, increasing B_4C with MoS_2 particles in the composite will result in a delay in the occurrence of hits. Fig. 12 explains the time vs amplitude line graph for all reinforcement. Crack initiation takes longer with the addition of B_4C and MoS_2. The amplitude for reinforcement particle has increased to a maximum of 5217 dB for Al8011-12%B_4C-2%MoS_2 reinforcement. Therefore, it is conferment that the material has high strength with an increase in reinforcement material compared to pure alloy. The same trends have been noted by many other researchers [12, 21,25].

3.4. Corrosion analysis through the immersion method

The calculated corrosion rate (Cr) value is plotted in the graph shown in Fig. 13. The matrix material (Al8011 alloy) has maximum corrosion and the rate of mass loss is 0.054 mm/yr at 250 Hours. The aluminium alloy exposed to any corrosive environment will form a passive film and protects the material from degradation. With the composition of 3%-12% B_4C with 2% MoS_2 added to the matrix Al8011, the corrosion resistance was reduced over varying periods. The corrosion rate of mass loss is 0.024725 mm/yr, 0.019781 mm/yr, 0.018955 mm/yr and 0.016262 mm/yr at 250 hours respectively. When the oxide scale thickness increase, the passive film breaks and corrosion due to pitting or crevice were observed. These corrosion phenomena are controlled with a proper manufacturing process. However, while adding the reinforcement with aluminium matrix the properties of the material inherently change. The presence of B_4C and MoS_2 in the aluminium alloy will help to avoid pitting or crevice corrosion in the early stage and protects the material. In the proposed research the increase in weight percentage found a decrease in corrosion resistance. That is the presence of reinforcement particles reacting with the corrosive medium has initiated corrosion and mass loss increased. Therefore, the increased weight percentage of reinforcement particles isrecommended for making Al8011 metal matrix composite. Other researchers have observed similar trends [23,33].

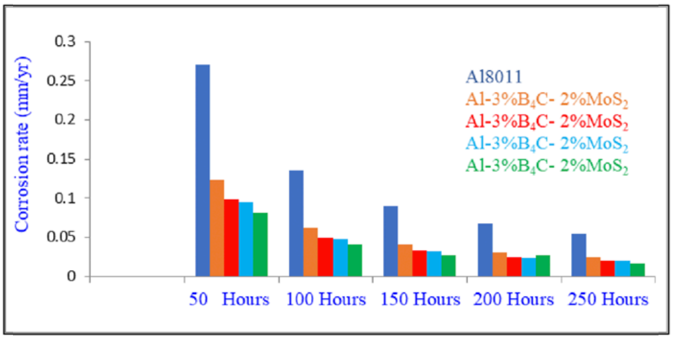

Fig. 13. The corrosion rate of the composite samples immersed in seawater

4. Conclusions

The investigation is performed to develop aluminium matrix composite with Boron carbide and molybdenum disulfide at different weight proportions. The composite developed is subjected to different mechanical testing of materials following ASTM standards. From the results, the following points are conclusions

- The density of the composite was found to decrease with the addition of B_4C and MoS_2. The Al8011-12%B_4C-2% MoS_2 possesses minimum theoretical density, actual density and porosity as compared with other composites. It is also confirmed that the Al8011-12%B_4C-2% MoS_2 has better metallurgical bonding with less porosity.

- The tensile strength of the composite is measured with axial loading assisted by the AE system. Al8011-12%B_4C-2% MoS_2 has a maximum strength of 161 MPa (0.161 kN/mm^2).
- Overall performance of the axially loaded sample is correlated with the AE report. The AE report shows the influence of mechanical load in terms of amplitude. An increase in strength concerning the reinforcement weight percentage is identified to substantiate the actual findings.
- The fracture mechanism on the loaded sample revealed a regular ductile fracture. The soft matrix under pure ductile fracture is reflected with a dimple profile. The microstructure region with a fine dispersion of reinforcement revealed the ductile-brittle transition over axial loading.
- The corrosion rate of the developed composite has less compared to the base metal. The higher B_4C content with constant MoS_2 composites exhibits excellent corrosion resistance. MoS_2 supportsforming a passive film with molybdenum. However, the presence of sulfide does not support to formation protective layer.
- Therefore, based on the mechanical strength and the electrochemical behaviour of the Al8011 matrix with 12%B_4C and 2% MoS_2 reinforced composite has performed better than the other combination. Hence, it is recommended to develop the proposed composite for real-time application.

REFERENCES

[1] Bhargavi Rebba, N. Ramanaiah, Investigations on Mechanical Behaviour of B_4C and MoS_2 Reinforced AA2024 Hybrid Composites, J. Manuf. Sci. Prod. **15**, l 339-343 (2015).

[2] S. Ajith Arul Daniel, D. Sakthivel, P.M. Sudhagar, Gopal, Study on Tribological behaviour of Al/SiC/MoS_2 hybrid metal matrix composites in high temperature environmental condition, Silicon **10**, 2129-2139 (2018). DOI: https://doi.org/10.1007/s12633-017-9739-2

[3] S. Suresha, B.K. Sridhara, Wear characteristics of hybrid aluminium matrix composites reinforced with graphite and silicon carbide particulates, Compos. Sci. Technol. **70**, 1652-1659 (2010). DOI: https://doi.org/10.1016/j.compscitech.2010.06.013

[4] B. Latha Shankar, K.C. Anil, P.J. Karabasappagol, Study on Effect of Graphite Particles on Tensile, Hardness and Machinability of Aluminium 8011 Matrix Material, Mater. Sci. Eng. **149**, 012060 (2016). DOI: https://doi.org/10.1088/1757-899X/149/1/012060

[5] K.V. Sreenivasrao, K.C. Anil, K.G. Girish, Akash, Mechanical characterization of red mud reinforced Al8011 matrix composite, ARPN J. Eng. Appl. Sci. **11**, 229-234 (2016).

[6] N. Saini, C. Pandey, S. Thapliyal, D.K. Dwivedi, Mechanical properties and Wear behavior of Zn and MoS_2 reinforced surface composite Al-Si alloys using friction stir processing, Silicon **10**, 1979-1990 (2018). DOI: https://doi.org/10.1007/s12633-017-9710-2

[7] Harun Mindivan, Reciprocal sliding wear behaviour of B_4C particulate reinforced aluminum alloy composites, Mater. Lett. **64**, 405-407 (2010). DOI: https://doi.org/10.1016/j.matlet.2009.11.032

[8] Suswagata Poria, Prasanta Sahoo, Goutam Sutradhar, Tribological characterization of stir-cast aluminium-TiB_2 metal matrix composites, Silicon **8**, 591-599 (2016). DOI: https://doi.org/10.1007/s12633-016-9437-5

[9] K. Soorya Prakash, R. Sathiya Moorthy, P.M. Gopal, V. Kavimani, Effect of reinforcement, compact pressure and hard ceramic coating on aluminium rock dust composite performance, Int. J. Refract. Metals. Hard Mater. **54**, 223-229 (2016). DOI: https://doi.org/10.1016/j.ijrmhm.2015.07.037

[10] M. Uthayakumar, S. ThirumalaiKumaran, M. AdamKhan, S. Skoczypiec, W. Bizon, Microdrilling of AA (6351)-SiC-B_4C Composite Using Hybrid Micro-ECDM Process, J. Test. Eval. **48** (2018). DOI: https://doi.org/10.1520/JTE20180216

[11] C. Emmy Prema, S. Suresh, G. Ramanan, M. Sivaraj, Characterization, corrosion and failure strength analysis of Al7075 influenced with B_4C and Nano-Al_2O_3 composite using online acoustic emission, Mater. Res. Express. **7**, 016524 (2020). DOI: https://doi.org/10.1088/2053-1591/ab6257

[12] C.M. Anand Partheeban, M. Rajendran, S.C. Vettivel, S. Suresh, N.S.V. Moorthi, Mechanical behaviour and failure analysis using online acoustic emission on nano-graphite reinforced Al6061-10TiB_2 hybrid composite using powder metallurgy, Mat. Sci. and Eng. A **632**, 1-13 (2015). DOI: http://dx.doi.org/10.1016/j.msea.2015.02.064

[13] M. Navaneetha Krishnan, S. Suresh, S.C. Vettivel, Characterization, formability, various stresses and failure analysis on workability of sintered Mg-5%B_4C composite under triaxial stress state condition, J. of Alloys Compd. **747**, 324-339 (2018). DOI: https://doi.org/10.1016/j.jallcom.2018.02.320

[14] S. Suresh, M. Navaneetha Krishnan, S.C. Vettivel. Effect of B_4C on strength coefficient, cold deformation and work hardening exponent characteristics of Mg composites, J. Magnes. Alloy, (2020). DOI: https://doi.org/10.1016/j.jma. 2020.09.010

[15] Shoufa Liu, Yinwei Wang, T. Muthuramalingam, G. Anbuchezhiyan, Effect of B_4C and MoS_2 reinforcement on micro structure and wear properties of aluminum hybrid composite for automotive applications, Compos. B. Eng. (2019). DOI: https://doi.org/10.1016/j.compositesb.2019.107329

[16] J.S. David Joseph, B. Kumaragurubaran, S. Sathish, Effect of MoS_2 on the Wear Behavior of Aluminium (AlMg0.5Si) Composite, Silicon **12**, 1481-1489 (2020). DOI: https://doi.org/10.1007/s12633-019-00238-x

[17] Donghyun Lee, Junghwan Kim, Sang-Kwan Lee, Yangdo Kim, Sang-Bok Lee, Seungchan Cho, Experimental and thermodynamic study on interfacial reaction of B4CeAl6061 composites fabricated by stir casting process, J. of Alloys. Compd. **859**, 157813 (2021). DOI: https://doi.org/10.1016/j.jallcom.2020.157813

[18] J. Hashim, L. Looney, M.S.J. Hashmi, Particle distribution in cast metal matrix composites Part I, J. Mater. Process. Technol. **123**, 251-257 (2002). PII: S0924 - 0136(02)00098-5

[19] M. Saravana Kumar, S. Rashia Begum, C.I. Pruncu, Mehdi Shahedi Asl, Role of homogeneous distribution of SiC reinforcement

on the characteristics of stir casted Al-SiC composites, J. Alloys. Compds. **869**, 159250 (2021).
DOI: https://doi.org/10.1016/j.jallcom.2021.159250

[20] M. Ying Zhang, Yue Li, Huan Sheng Lai, Chunmei Bai, Kang Lin Liu, Acoustic Emission Response and Damage Process for Q235 Steel in an in Situ Tensile Test, Archives of Acoustics **44**, 807-813, (2019).

[21] S. Suresh, N. Shenbaga Vinayaga Moorthi, S.C. Vettivel, N. Selvakumar, G.R. Jinu, Effect of graphite addition on mechanical behavior of Al6061/TiB_2 hybrid composite using acoustic emission, Mater. Sci. Eng. A **612**16-27(2014).
DOI: http://dx.doi.org/10.1016/j.msea.2014.06.024

[22] ASM International, Metal handbook: Non – destructive evaluation and quality control, Volume **9**, ASM International, Ohio, (1995).

[23] Pabitra Maji, Rahul Kanti Nath, Pritam Paul, R.K. Bhogendro Meitei, Subrata Kumar Ghosh, Effect of processing speed on wear and corrosion behavior of novel MoS_2 and CeO_2 reinforced hybrid aluminum matrix composites fabricated by friction stir processing, J. Manuf. Process. **69**, 1-11 (2021).
DOI: https://doi.org/10.1016/j.jmapro.2021.07.032

[24] Manivannan, S. Ranganathan, S. GopalaKannan, Mechanical Properties and Tribological Behavior of Al6061-SiC-Gr Self-Lubricating Hybrid Nanocomposites, Trans. Indian Inst. Met. (2018). DOI: https://doi.org/10.1007/s12666-018-1321-0

[25] M. Navaneetha Krishnan, S. Suresh, S.C. Vettivel, C. Emmy Prema, C.P. Jesuthanam, A Novel Image Processing Technique for Analyzing Wear Worn Surface Roughness and Corrosion Behavior of Sintered Mg/B_4C Composites, Trans. Indian Inst. Met. (2020).
DOI: https://doi.org/10.1007/s12666-020-02123-3

[26] S. Suresh, N. Shenbaga Vinayaga Moorthi, C. Emmy Prema, Tribological and Mechanical behavior study of Al6061-TiB_2 Metal Matrix Composites using Stir Casting, Adv. Mat. Res. **984-985**, 200-206 (2014). DOI: https://doi.org/10.4028/www.scientific.net/AMR.984-985.200

[27] Song-Jeng Huang, Murugan Subramani, Dawit Bogale Alemayehu, The effect of micro-SiCp content on the tensile and fatigue behavior of AZ61 magnesium alloy matrix composites, Int. J. Met. **15**, 780-793 (2021).
DOI: https://doi.org/10.1007/s40962-020-00508-0

[28] M. Navaneetha Krishnan, S. Suresh, S.C. Vettivel, Effects on Micro-Surface Texturing of Mg/B_4C Matrix Composites Under Dry Sliding Wear Condition, Trans. Indian Inst. Met. (2020).
DOI: https://doi.org/10.1007/s12666-020-01913-z

[29] N.G. Siddesh Kumar, R. Suresh, G.S. Shiva Shankar, High Temperature Wear Behavior of Al2219/n-B_4C/MoS_2 Hybrid Metal Matrix Composites, Compos. Commun. **19**, 1-73 (2020).

[30] T.J. Holroyd, The acoustic emission and ultrasonic monitoring handbook, Coxmoor Publishing Company, UK, (2000).

[31] Hiroshi Kato, Shota Otsuka, Akitoshi Nonaka, Influence of casting defects on fatigue properties of SiC particulate dispersed aluminum alloy composite castings, Mater. Sci. Eng. A **560**, 717-726 (2013). DOI: http://dx.doi.org/10.1016/j.msea.2012.10.019

[32] Mehrdad Zolfaghari, Mohammad Azadi, characterization of high-cycle bending fatigue behaviors for piston aluminum matrix SiO_2 nano-composites in comparison with aluminum-silicon alloys, Int. J. Met. (2020).
DOI: https://doi.org/10.1007/s40962-020-00437-y

[33] M. Sambathkumar, P. Navaneethakrishnan, K.S.K. Sasikumar, R. Gukendran, K. Ponappa, Investigation of Mechanical and Corrosion Properties of Al 7075/Garnet Metal Matrix Composites by Two-stage Stir Casting Process, Arch. Metall. Mater. **66**, 4, 1123-1129 (2021).
DOI: https://doi.org/10.24425/amm.2021.136432